Antitumor activities of anti-CD44 monoclonal antibodies in mouse xenograft models of esophageal cancer

KENICHIRO ISHIKAWA[1,2], HIROYUKI SUZUKI[1], TOMOKAZU OHISHI[3,4], TAKURO NAKAMURA[1], MIYUKI YANAKA[1], GUANJIE LI[1], TOMOHIRO TANAKA[1], AKIRA OHKOSHI[2], MANABU KAWADA[4], MIKA K. KANEKO[1], YUKIO KATORI[2] and YUKINARI KATO[1]

[1]Department of Antibody Drug Development, Tohoku University Graduate School of Medicine, Aoba-ku, Sendai, Miyagi 980-8575, Japan; [2]Department of Otolaryngology, Head and Neck Surgery, Tohoku University Graduate School of Medicine, Aoba-ku, Sendai, Miyagi 980-8575, Japan; [3]Institute of Microbial Chemistry (BIKAKEN), Numazu, Microbial Chemistry Research Foundation, Numazu, Shizuoka 410-0301, Japan; [4]Institute of Microbial Chemistry (BIKAKEN), Laboratory of Oncology, Microbial Chemistry Research Foundation, Shinagawa-ku, Tokyo 141-0021, Japan

Received April 18, 2024; Accepted July 23, 2024

DOI: 10.3892/or.2024.8806

Abstract. CD44 is a type I transmembrane glycoprotein associated with poor prognosis in various solid tumors. Since CD44 plays a critical role in tumor development by regulating cell adhesion, survival, proliferation and stemness, it has been considered a target for tumor therapy. Anti-CD44 monoclonal antibodies (mAbs) have been developed and applied to antibody-drug conjugates and chimeric antigen receptor-T cell therapy. Anti-pan-CD44 mAbs, C_{44}Mab-5 and C_{44}Mab-46, which recognize both CD44 standard (CD44s) and variant isoforms were previously developed. The present study generated a mouse IgG_{2a} version of the anti-pan-CD44 mAbs (5-mG_{2a} and C_{44}Mab-46-mG_{2a}) to evaluate the antitumor activities against CD44-positive cells. Both 5-mG_{2a} and C_{44}Mab-46-mG_{2a} recognized CD44s-overexpressed CHO-K1 (CHO/CD44s) cells and esophageal tumor cell line (KYSE770) in flow cytometry. Furthermore, both 5-mG_{2a} and C_{44}Mab-46-mG_{2a} could activate effector cells in the presence of CHO/CD44s cells and exhibited complement-dependent cytotoxicity against both CHO/CD44s and KYSE770 cells. Furthermore, the administration of 5-mG_{2a} and C_{44}Mab-46-mG_{2a} significantly suppressed CHO/CD44s and KYSE770 xenograft tumor development compared with the control mouse IgG_{2a}. These results indicate that 5-mG_{2a} and C_{44}Mab-46-mG_{2a} could exert antitumor activities against CD44-positive cancers and be a promising therapeutic regimen for tumors.

Correspondence to: Dr Yukinari Kato, Department of Antibody Drug Development, Tohoku University Graduate School of Medicine, 2-1, Seiryo-machi, Aoba-ku, Sendai, Miyagi 980-8575, Japan
E-mail: yukinari.kato.e6@tohoku.ac.jp

Abbreviations: CD44s, CD44 standard; CD44v, CD44 variant; HA, hyaluronic acid; mAb, monoclonal antibody; ADCC, antibody-dependent cellular cytotoxicity; CDC, complement-dependent cytotoxicity; FcγR, Fcγ receptor; CAR, chimeric antigen receptor; FUT8, fucosyl-transferase 8; CHO, Chinese hamster ovary; CBIS, Cell-Based Immunization and Screening; ESCC, esophageal squamous cell carcinoma; PBS, phosphate-buffered saline

Key words: CD44, mAb, ADCC, CDC, esophageal tumor, antitumor activity

Introduction

Overexpression of CD44 is observed in various solid tumors, which are involved in the tumor malignant progression through the promotion of cellular proliferation, invasiveness and stemness via specific signaling pathways (1). The diversity of CD44 molecular function is mediated by the alternative splicing (2). CD44 is encoded in 20 exons. The first five (1-5) and the last five (16-20) are constant exons that generate the shortest CD44 standard (CD44s) isoform. The exons 6-15 are alternatively spliced and inserted into the CD44s as variant exons (3). The CD44 splice variants with variant exons are designated CD44 variant (CD44v) isoforms. The inclusion of CD44v exons in various combinations is regulated by receptor tyrosine kinase signaling and splicing activators of pre-mRNA (1).

CD44 possesses an extracellular domain (ectodomain), a transmembrane domain, and an intracellular cytoplasmic domain (4). The ectodomain contains a hyaluronic acid (HA)-binding domain (HABD) that mediates cellular homing, adhesion, migration and proliferation (4). Both CD44s and CD44v isoforms have the HABD, and the HA binding causes conformational changes of the CD44, which results in the promotion of intracellular signaling pathways to regulate cell migration and proliferation (5). In CD44v isoforms, the variant exons-encoding sequences form the stem region, which provides a co-receptor for various growth factors and cytokines. These functions activate specific signaling pathways to promote invasion and stemness (6). Therefore, different isoforms of CD44v exhibit different functions according to the inserted variant exons in the CD44 ectodomain.

The relationship between CD44 expression and prognosis in patients with cancer has been evaluated and showed both poor and favorable outcomes (7). Currently, increased evidence suggests that overexpression of CD44 and its isoforms is an unfavorable indicator in patients with cancer (7). In an analysis of multiple studies, including 583 pancreatic cancer cases, overexpression of CD44 was predictive of poor overall survival, a more advanced stage and more lymph node invasion (8). Furthermore, another meta-analysis investigated the prognostic significance of cancer stem cell markers, including CD44, from 52 studies of ovarian cancer. The study concluded that CD44 overexpression was predictive of worse disease-free survival and resistance to chemotherapy (9).

Several anti-CD44 monoclonal antibodies (mAbs) have been developed for preclinical and clinical research for tumor therapy. An anti-pan-CD44 mAb (H4C4) reduced tumor growth, metastasis and post-radiation recurrence in a human pancreatic tumor xenograft model (10). A humanized anti-pan-CD44 mAb, RG7356, showed the cytotoxicity for B cell leukemia but no cytotoxicity on normal B cells. Administration of RG7356 to immunodeficient mice engrafted with chronic lymphocytic leukemia cells resulted in complete clearance of engrafted leukemia cells (11). Phase I clinical trials with RG7356 were conducted in patients with acute myeloid leukemia (12) and advanced CD44-positive solid tumor patients (13). Although RG7356 showed an acceptable safety profile, the studies were not continued due to the lack of a clinical and/or pharmacodynamic dose-response relationship with RG7356 (13).

Therapies using anti-CD44v6 mAbs were considered since CD44v6 plays critical roles in the malignant progression of tumors (14). Humanized anti-CD44v6 mAbs, including BIWA-4 and BIWA-8, were developed. These mAbs labeled with ^{186}Re were evaluated in head and neck squamous cell carcinoma xenograft-bearing mice and exhibited therapeutic efficacy (15). Furthermore, the BIWA-4 was developed into a humanized version-drug conjugate, bivatuzumab-mertansine (anti-tubulin agent), which was evaluated in clinical trials (16). However, the clinical trials were terminated because of the severe skin toxicity, such as lethal epidermal necrolysis (17). Since CD44v6 is expressed in normal skin epithelium, the toxicity of mertansine in the skin was most likely responsible for the high toxicity (17,18). Previously, a mutated version of BIWA-4, called BIWA-8, was developed for increasing binding affinity by two amino acid substitutions of the light chain (15). The BIWA-8 was further developed to chimeric antigen receptors (CARs). The BIWA-8 CAR-T showed antitumor activities against multiple myeloma or acute myeloid leukemia engrafted with immunodeficient mice (19). Furthermore, the BIWA-8 CAR-T exhibited efficacy in lung and ovarian carcinomas xenograft models (20), which is expected for an application toward solid tumors.

In our previous studies, an anti-pan-CD44 mAb, C_{44}Mab-5 (IgG_1, kappa) was developed using the Cell-Based Immunization and Screening (CBIS) method (21). Another mAb (C_{44}Mab-46) (22) was created by immunization of the CD44v3-10 ectodomain. Both C_{44}Mab-5 and C_{44}Mab-46 have the epitopes within the constant exon 2- and 5-encoded sequences (23-25) and could be applied to immunohistochemistry in oral squamous cell carcinoma (21) and esophageal squamous cell carcinoma (ESCC) (22), respectively. Furthermore, various anti-CD44v mAbs have been developed, such as C_{44}Mab-6 (an anti-CD44v3 mAb) (26), C_{44}Mab-108 (an anti-CD44v4 mAb) (27), C_{44}Mab-3 (an anti-CD44v5 mAb) (28), C_{44}Mab-9 (an anti-CD44v6 mAb) (29), C_{44}Mab-34 (an anti-CD44v7/8 mAb) (30), C_{44}Mab-1 (an anti-CD44v9 mAb) (31) and C_{44}Mab-18 (an anti-CD44v10 mAb) (32). The combinational use of the anti-CD44 mAbs is essential for comprehensively analyzing human tumors.

In the present study, a mouse IgG_{2a} type of recombinant C_{44}Mab-5 (5-mG_{2a}) and C_{44}Mab-46 (C_{44}Mab-46-mG_{2a}) was produced using fucosyl-transferase 8 (FUT8)-deficient ExpiCHO-S cells and the antitumor activity in xenograft-bearing mice was investigated.

Materials and methods

Cell lines. ESCC cell line KYSE770 was obtained from the Japanese Collection of Research Bioresources. Chinese hamster ovary (CHO)-K1 was obtained from the American Type Culture Collection. CHO/CD44s was previously established by transfecting pCAG-Ble/PA16-CD44s into CHO-K1 cells (22). KYSE770 was cultured in Dulbecco's Modified Eagle's Medium (DMEM; Nacalai Tesque, Inc.) supplemented with 10% (v/v) heat-inactivated fetal bovine serum (FBS; Thermo Fisher Scientific, Inc.), 0.25 μg/ml amphotericin B, 100 μg/ml streptomycin, and 100 U/ml penicillin (Nacalai Tesque, Inc.). CHO-K1 was cultured in Roswell Park Memorial Institute (RPMI)-1640 medium (Nacalai Tesque, Inc.) supplemented with 10% (v/v) FBS, 0.25 μg/ml amphotericin B, 100 μg/ml streptomycin and 100 U/ml penicillin (RPMI-1640 complete medium). CHO/CD44s were cultured in RPMI-1640 complete medium containing 0.5 mg/ml Zeocin (InvivoGen). All cells were cultured in a humidified incubator at 37˚C with 5% CO_2.

Antibodies. Anti-pan-CD44 mAbs, C_{44}Mab-5 and C_{44}Mab-46 were previously established (21,22). To generate recombinant mAbs, V_H cDNAs of C_{44}Mab-5 or C_{44}Mab-46 and C_H of mouse IgG_{2a} were cloned into the pCAG-Ble vector (FUJIFILM Wako Pure Chemical Corporation). V_L cDNA of C_{44}Mab-5 or C_{44}Mab-46 and C_L cDNA of mouse kappa light chain were also subcloned into the pCAG-Neo vector (FUJIFILM Wako Pure Chemical Corporation). The vectors were transduced into BINDS-09 (FUT8-knockout ExpiCHO-S) cells (33). 5-mG_{2a} and C_{44}Mab-46-mG_{2a} were purified using Ab-Capcher (ProteNova Co., Ltd.). 281-mG_{2a} (an anti-hamster podoplanin mAb, control mouse IgG_{2a}) was previously described (34).

Flow cytometry. The cells, obtained using 0.25% trypsin and 1 mM ethylenediamine tetraacetic acid (EDTA; Nacalai Tesque, Inc.), were treated with 5-mG_{2a} and C_{44}Mab-46-mG_{2a}, or control blocking buffer [phosphate-buffered saline (PBS) containing 0.1% bovine serum albumin (Nacalai Tesque, Inc.)] for 30 min at 4˚C. Subsequently, the cells were treated with anti-mouse IgG conjugated with Alexa Fluor 488 (1:2,000; Cell Signaling Technology, Inc.) for 30 min at 4˚C. Fluorescence data were collected using the SA3800 Cell Analyzer (Sony Corp.) and analyzed using SA3800 software ver. 2.05 (Sony Corp.).

Antibody-dependent cellular cytotoxicity (ADCC) reporter bioassay. An ADCC Reporter Bioassay kit (Promega Corporation) was used for the ADCC reporter bioassay. The human FcγRIIIa receptor and a nuclear factor of activated T-cells (NFAT) response element driving firefly luciferase-expressed Jurkat cells were used as effector cells. The target CHO/CD44s and KYSE770 cells (12,500 cells per well) were seeded into a 96-well white solid plate. The serially diluted 5-mG_{2a} and C_{44}Mab-46-mG_{2a} were added to the target cells. The effector cells (75,000 cells in 25 μl) were then added and co-cultured with antibody-treated target cells at 37˚C for 6 h. Luminescence was measured with a GloMax luminometer (Promega Corporation).

Complement-dependent cytotoxicity (CDC). The target CHO/CD44s and KYSE770 cells were labeled using 10 μg/ml Calcein AM (Thermo Fisher Scientific, Inc.). The target cells ($1x10^4$ cells/well) were mixed with 100 μg/ml of control 281-mG_{2a}, 5-mG_{2a}, or C_{44}Mab-46-mG_{2a} and rabbit complement (final dilution 1:10, Low-Tox-M Rabbit Complement; Cedarlane Laboratories). The calcein release to the medium was measured after a 4-h incubation. The maximum fluorescence of the medium was also measured after lysing all cells with a buffer containing 0.5% Triton X-100, 10 mM Tris-HCl (pH 7.4), and 10 mM EDTA. Cytotoxicity (% of lysis) was calculated as % lysis=(E-S)/(M-S) x100. E is the fluorescence of combined target and effector cells. S is the spontaneous fluorescence of target cells only. M is the maximum fluorescence measured. Statistical analyses were performed using GraphPad PRISM 6 software (GraphPad Software, Inc.; Dotmatics).

Antitumor activity of 5-mG_{2a} and C_{44}Mab-46-mG_{2a} in xenografts of CHO/CD44s and KYSE770. All animal experiments were performed following regulations and guidelines to minimize animal distress and suffering in the laboratory by the Institutional Committee for Experiments of the Institute of Microbial Chemistry (Numazu, Japan). The animal study protocol was approved (approval nos. 2023-037 and 2023-054) by the Institutional Committee for Experiments of the Institute of Microbial Chemistry (Numazu, Japan). BALB/c nude mice (5-week-old female, a total of 72 mice) were purchased from Jackson Laboratories, Inc. and maintained on an 11-h light/13-h dark cycle at a temperature of 23±2˚C and 55±5% humidity in a specific pathogen-free environment, across the experimental period. Food and water were supplied *ad libitum*. The weight of the mice was monitored twice per week and their health was monitored three times per week. CHO/CD44s and KYSE770 cells ($5x10^6$ cells) suspended with BD Matrigel Matrix Growth Factor Reduced (BD Biosciences) were inoculated into the left flank of the mice subcutaneously. On day 7 after the inoculation, 100 μg of 5-mG_{2a} (n=8), C_{44}Mab-46-mG_{2a} (n=8), or control 281-mG_{2a} (n=8) in 100 μl PBS were injected intraperitoneally. Additional antibody injections were performed on days 14 and 21. The tumor volume was measured on days 7, 9, 14, 17, 21 and 23. In the KYSE770 xenograft experiment (500 μg dosage), 500 μg of 5-mG_{2a} (n=8), C_{44}Mab-46-mG_{2a} (n=8), or control 281-mG_{2a} (n=8) in 100 μl PBS were injected intraperitoneally on days 8 and 13 after the inoculation. The tumor volume was measured on days 8, 12, and 19. The tumor volume was calculated using the formula: Volume=W^2 x L/2, where W is the short diameter and L is the long diameter. The loss of original body weight was determined to a point >25% (35) and/or a maximum tumor size >3,000 mm^3 and/or significant changes in the appearance of tumors as humane endpoints for euthanasia. Cervical dislocation was used for euthanasia. Mice death was confirmed by respiratory arrest and rigor mortis. The xenograft tumors were carefully removed from the sacrificed mice and weighed immediately.

Immunohistochemical analysis. The paraffin-embedded xenograft tumors were autoclaved in citrate buffer (pH 6.0; Nichirei Biosciences, Inc.) for 20 min. After blocking with SuperBlock T20 (Thermo Fisher Scientific, Inc.), sections (4 μm) were incubated with 1 μg/ml of C_{44}Mab-46 and mPMab-1 [a mouse-rat chimeric antibody against mouse podoplanin (36)] for 1 h at room temperature and then treated with the EnVision+ Kit for mouse (Agilent Technologies, Inc.) for 30 min. The color was developed using 3,3'-diaminobenzidine tetrahydrochloride (DAB; Agilent Technologies, Inc.). Counterstaining was performed with hematoxylin (Merck KGaA). Hematoxylin and eosin (H&E) staining was performed using hematoxylin and eosin (FUJIFILM Wako Pure Chemical Corporation). Leica DMD108 fluorescence microscope (Leica Microsystems GmbH) was used to examine the sections and obtain images.

Statistical analyses. All data are expressed as the mean ± standard error of the mean (SEM). Two-way ANOVA with Tukey's multiple comparisons test and two-way ANOVA with Sidak's multiple comparisons tests were conducted in CDC and tumor weight measurement, respectively. Two-way ANOVA with Sidak's multiple comparisons test was utilized for tumor volume and mice weight. GraphPad Prism 6 (GraphPad Software, Inc.; Dotmatics) was used for all calculations. $P<0.05$ was considered to indicate a statistically significant difference.

Results

Flow cytometric analysis against CHO/CD44s and KYSE770 cells using 5-mG_{2a} and C_{44}Mab-46-mG_{2a}. In our previous study, anti-pan-CD44 mAbs (C_{44}Mab-5 and C_{44}Mab-46) were established and were shown to be available for flow cytometry and immunohistochemistry (21,22). In the present study, a mouse IgG_{2a} type of C_{44}Mab-5 and C_{44}Mab-46 (5-mG_{2a} and C_{44}Mab-46-mG_{2a}) were produced by combining V_H and V_L of both mAbs with C_H and C_L of mouse IgG_{2a}, respectively (Fig. 1A). The reactivity of CD44s-overexpressed CHO-K1 cells (CHO/CD44s) and an endogenous CD44-expressing esophageal tumor cell line (KYSE770) was first confirmed. 5-mG_{2a} and C_{44}Mab-46-mG_{2a} detected CHO/CD44s in a concentration-dependent manner (Fig. 1B), but did not detect parental CHO-K1 cells (negative control, Fig. S1). 5-mG_{2a} and C_{44}Mab-46-mG_{2a} also detected KYSE770 cells in a concentration-dependent manner (Fig. 1C). KYSE770 cells were also recognized by anti-CD44v mAbs including C_{44}Mab-6 (an anti-CD44v3 mAb), C_{44}Mab-3 (an anti-CD44v5 mAb), C_{44}Mab-9 (an anti-CD44v6 mAb), and C_{44}Mab-18 (an anti-CD44v10 mAb) (Fig. S2). These results indicated that 5-mG_{2a} and C_{44}Mab-46-mG_{2a} recognize exogenous and endogenous CD44.

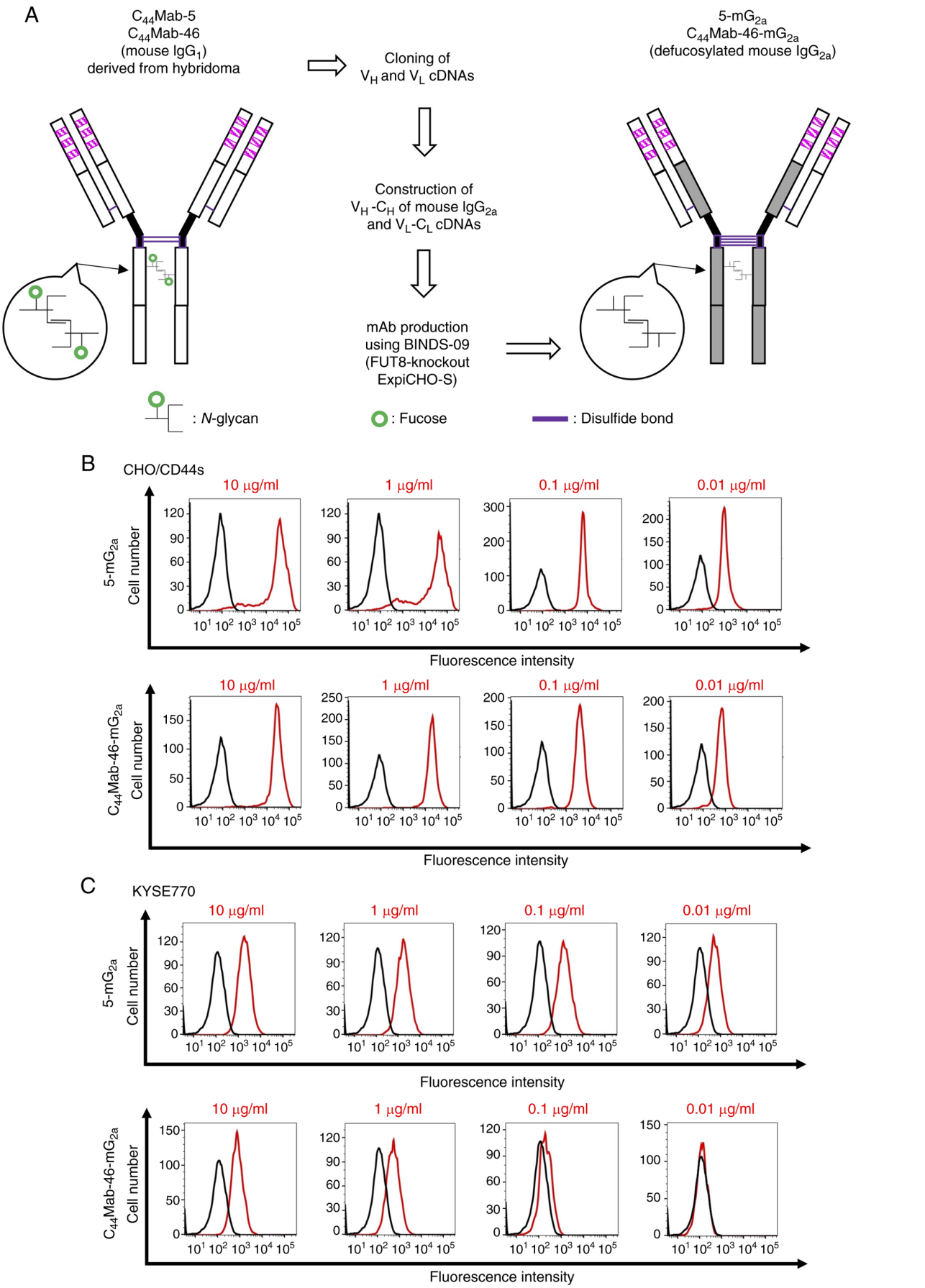

Figure 1. Flow cytometry using 5-mG_{2a} and C_{44}Mab-46-mG_{2a}. (A) Class-switched and defucosylated mouse IgG_{2a} mAbs, 5-mG_{2a} and C_{44}Mab-46-mG_{2a}, were generated from C_{44}Mab-5 and C_{44}Mab-46 (mouse IgG_1), respectively. (B) CHO/CD44s and (C) KYSE770 cells were treated with 10-0.01 μg/ml of 5-mG_{2a} and C_{44}Mab-46-mG_{2a} (red) or buffer control (black), followed by Alexa Fluor 488-conjugated anti-mouse IgG. Fluorescence data were analyzed using the SA3800 Cell Analyzer. mAb, monoclonal antibody.

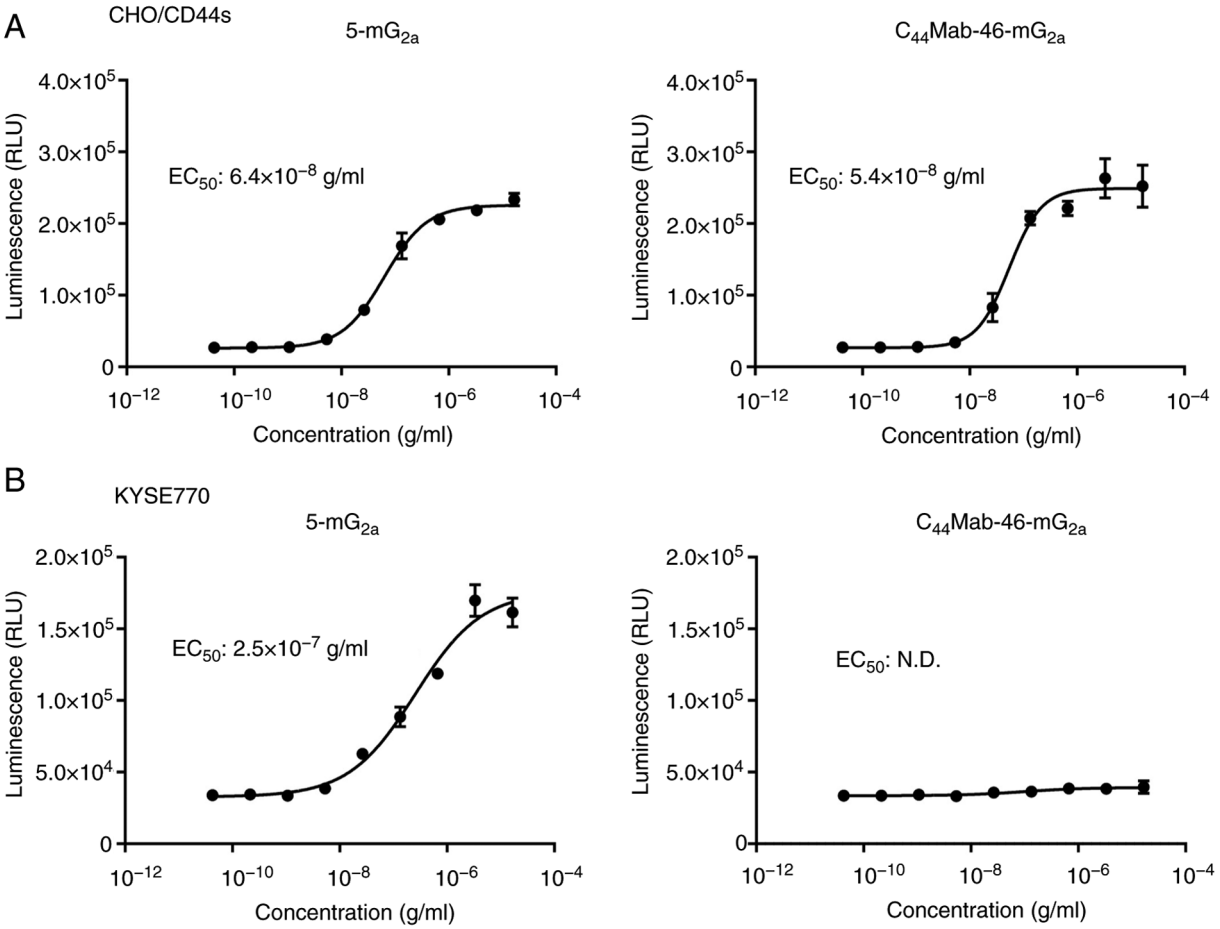

Figure 2. Evaluation of ADCC activity. The ADCC reporter assay by 5-mG_{2a} and C_{44}Mab-46-mG_{2a} in the presence of (A) CHO/CD44s and (B) KYSE770 cells. Values are presented as the mean ± SD. N.D., not determined; ADCC, antibody-dependent cellular cytotoxicity; mAb, monoclonal antibody.

5-mG_{2a} and C_{44}Mab-46-mG_{2a}-mediated ADCC pathway activation in the presence of CHO/CD44s and KYSE770 cells. To compare the ADCC pathway activation by 5-mG_{2a} and C_{44}Mab-46-mG_{2a}, the ADCC reporter bioassay was performed to measure the biological activity of the FcγRIIIa-mediated pathway activation by mAbs (37). CHO/CD44s cells were treated with diluted mAbs and then incubated with effector cells, which possess the human FcγRIIIa receptor and *Firefly* luciferase regulated by an NFAT response element. As demonstrated in Fig. 2A, 5-mG_{2a} and C_{44}Mab-46-mG_{2a} activated the effector in a concentration-dependent manner (EC_{50}; 6.4x10^{-8} g/ml and 5.4x10^{-8} g/ml, respectively). In the presence of KYSE770 cells, 5-mG_{2a} activated the effector (EC_{50}; 2.5x10^{-7} g/ml, Fig. 2B). However, C_{44}Mab-46-mG_{2a} did not (Fig. 2B).

The CDC by 5-mG_{2a} and C_{44}Mab-46-mG_{2a} against CHO/CD44s and KYSE770 cells. The CDC mediated by 5-mG_{2a} and C_{44}Mab-46-mG_{2a} against CHO/CD44s and KYSE770 cells was next examined. As shown in Fig. 3, both 5-mG_{2a} and C_{44}Mab-46-mG_{2a} significantly exerted CDC against CHO/CD44s cells (67 and 88% cytotoxicity, respectively) and KYSE770 (27 and 31% cytotoxicity, respectively) compared with those induced by control mouse IgG_{2a} (281-mG_{2a}). These results demonstrated that 5-mG_{2a} and C_{44}Mab-46-mG_{2a} exhibited potent CDC activities against CHO/CD44s and KYSE770 cells.

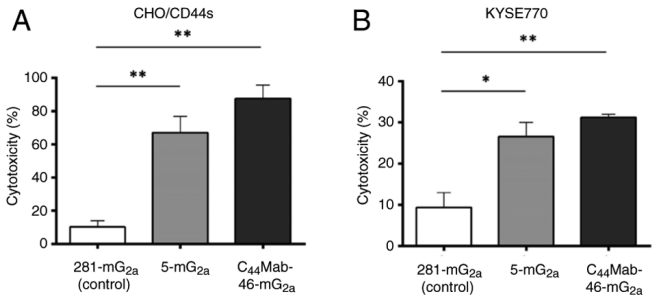

Figure 3. Evaluation of CDC activity by 5-mG_{2a} and C_{44}Mab-46-mG_{2a} against CHO/CD44s and KYSE770 cells. The CDC induced by 5-mG_{2a}, C_{44}Mab-46-mG_{2a}, or control mouse IgG_{2a} (281-mG_{2a}) against (A) CHO/CD44s and (B) KYSE770 cells. Values are shown as the mean ± SEM. *P<0.05 and **P<0.01; one-way ANOVA with Tukey's multiple comparisons test. CDC, complement-dependent cytotoxicity; mAb, monoclonal antibody.

Antitumor effects of 5-mG_{2a} and C_{44}Mab-46-mG_{2a} against CHO/CD44s xenograft. In the CHO/CD44s xenograft tumors, 100 μg of 5-mG_{2a}, C_{44}Mab-46-mG_{2a}, or control mouse IgG_{2a} were injected into mice intraperitoneally on days 7, 14 and 21, following CHO/CD44s inoculation. On days 7, 9, 14, 17, 21 and 23, the tumor volume was measured. The 5-mG_{2a} and C_{44}Mab-46-mG_{2a} administration resulted in a significant reduction in tumor volume on days 17 (P<0.05), 21 (P<0.01) and 23 (P<0.01) compared with that of the control mouse

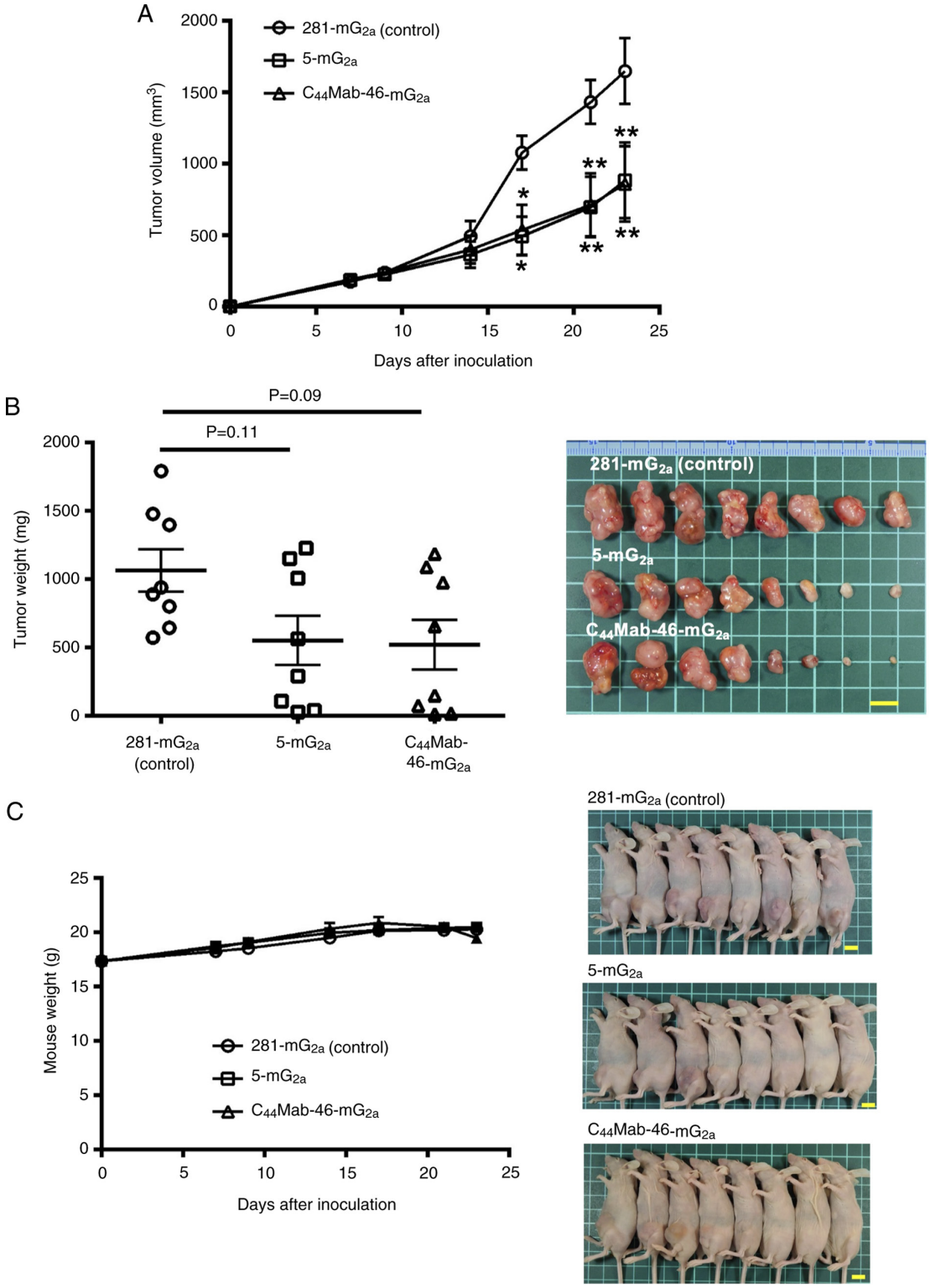

Figure 4. Antitumor activity of 5-mG_{2a} and C_{44}Mab-46-mG_{2a} against CHO/CD44s xenograft tumor. (A) Measurement of tumor volume in CHO/CD44s xenograft. CHO/CD44s cells ($5x10^6$ cells) were injected into mice subcutaneously. On day 7, 100 μg of 5-mG_{2a} and C_{44}Mab-46-mG_{2a} or control mouse IgG_{2a} (281-mG_{2a}) were injected into mice intraperitoneally. On days 14 and 21, additional antibodies were injected. On days 7, 9, 14, 17, 21 and 23 following the inoculation, the tumor volume was measured. Values are presented as the mean ± SEM. *P<0.05 and **P<0.01; two-way ANOVA with Sidak's multiple comparisons test. (B) The weight (left) and appearance (right) of excised CHO/CD44s xenografts on day 23. Values are presented as the mean ± SEM; one-way ANOVA with Tukey's multiple comparisons test. (C) The body weight (left) and appearance (right) of control mouse IgG2a, 5-mG2a, and C_{44}Mab-46-mG2a-treated mice. Scale bar, 1 cm. mAb, monoclonal antibody.

IgG_{2a} (Fig. 4A). The 5-mG_{2a} and C_{44}Mab-46-mG_{2a} administration resulted in 46 and 48% reductions in tumor volume compared with that of the control mouse IgG_{2a} on day 23, respectively. The histological analyses of tumors are demonstrated in Fig. S3. In the necrotic area of tumors, leukocytes and erythrocytes were infiltrated. Membranous staining of

CD44 in tumor and podoplanin-positive macrophage were also detected. However, a significant difference among control, 5-mG_{2a} and C_{44}Mab-46-mG_{2a}-treated tumors could not be observed.

The weight of CHO/CD44s tumors treated with 5-mG_{2a} and C_{44}Mab-46-mG_{2a} was lower than that of tumors treated with the control mouse IgG_{2a} (53 and 55% reduction, respectively; P=0.11 and P=0.09; Fig. 4B). Loss of body weight was not observed in the CHO/CD44s tumor-implanted mice during the treatments (Fig. 4C).

Antitumor effects of 5-mG_{2a} and C_{44}Mab-46-mG_{2a} on KYSE770 xenografts. In the KYSE770 xenograft models, 100 μg of 5-mG_{2a} and C_{44}Mab-46-mG_{2a} and control mouse IgG_{2a} were injected into mice on days 7, 14 and 21, following KYSE770 inoculation. Although the tendency of the reduction of tumor volume by the treatment with 5-mG_{2a} and C_{44}Mab-46-mG_{2a} was observed, significant differences were not obtained (Fig. S4). The dosage (500 μg) was next increased and the antitumor effects were investigated. As revealed in Fig. 5, 500 μg of 5-mG_{2a}, C_{44}Mab-46-mG_{2a} and control mouse IgG_{2a} were injected into mice on days 8 and 13, following KYSE770 inoculation. On days 8, 12 and 19, the tumor volume was measured. The 5-mG_{2a} and C_{44}Mab-46-mG_{2a} administration resulted in a significant reduction in tumor volume on day 19 (P<0.01) compared with that of the control mouse IgG_{2a} (Fig. 5A). The 5-mG_{2a} and C_{44}Mab-46-mG_{2a} administration resulted in 51 and 37% reduction of tumor volume compared with that of the control mouse IgG_{2a} on day 19, respectively. The histological analyses of tumors are demonstrated in Fig. S5. Membranous staining of CD44 in tumors and podoplanin-positive macrophages at the tumor periphery were observed. Infiltrated podoplanin-positive macrophages into tumors were not observed compared with KYSE770 xenograft.

The weight of KYSE770 tumors treated with 5-mG_{2a} and C_{44}Mab-46-mG_{2a} was significantly lower than that of tumors treated with the control mouse IgG_{2a} [47% (P<0.05) and 40% (P<0.05) reduction, respectively; Fig. 5B]. Loss of body weight was not observed in the KYSE770 tumor-implanted mice during the treatments (Fig. 5C).

Discussion

In the present study, mouse IgG_{2a} type anti-pan-CD44 mAbs (5-mG_{2a} and C_{44}Mab-46-mG_{2a}) was produced and antitumor activity against CHO/CD44s and KYSE770 xenograft tumors was evaluated. Although 5-mG_{2a} possesses superior affinity to CD44-expressing cells compared with C_{44}Mab-46-mG_{2a} (22,38), both 5-mG_{2a} and C_{44}Mab-46-mG_{2a} showed comparable ability of effector activation (Fig. 2A), CDC (Fig. 3A) and antitumor activity against CHO/CD44s (Fig. 4). Against KYSE770 cells, 5-mG_{2a} exhibited superior reactivity in flow cytometry (Fig. 1C) and effector activation (Fig. 2B) compared with C_{44}Mab-46-mG_{2a}. However, both mAbs showed similar antitumor activity to KYSE770 xenograft in high dosage (Fig. 5).

After the phase I trial of RG7356 in solid tumors, the developer Roche group reported that the CD44s expression is associated with HA production and predicts response to treatment with RG7356 in both xenograft tumor models and clinical response (39). The group also identified that overexpression of CD44s stimulates the HA production (39). These results suggest the close interplay between CD44s and HA and a potential biomarker to enrich patient responses to anti-CD44 mAb therapy in the clinic. In the present study, CD44s-overexpressed CHO-K1 cells and KYSE770 cells were used, which mainly express CD44v (Fig. S2) (22). Due to the lower levels of total CD44 (Fig. 1) and the CD44v expression in KYSE770 cells, a high dosage (500 μg) of mAbs was needed to suppress the KYSE770 xenograft.

As revealed in Fig. 2B, C_{44}Mab-46-mG_{2a} did not activate the effector cells in the presence of KYSE770 but exerted the antitumor effect *in vivo* (Fig. 5). The CDC is a crucial antitumor mechanism by mAbs (40,41). Some tendency was observed that C_{44}Mab-46-mG_{2a} showed a more significant CDC effect compared with 5-mG_{2a} (Fig. 3). The difference could be sufficient to exert similar antitumor effects *in vivo* by 5-mG_{2a} and C_{44}Mab-46-mG_{2a}. There was less infiltrated podoplanin-positive macrophage into KYSE770 xenograft compared with CHO/CD44 (Figs. S3 and S5). Since the infiltrated effector cells exert ADCC activity (42), this may be one of the reasons why ADCC did not contribute markedly in KYSE770 cells. One more possibility is their epitope. 5-mG_{2a} recognizes the N-terminal part of CD44 [amino acids 25-36, (25)], and C_{44}Mab-46-mG_{2a} recognizes the central part of CD44 [amino acids 174-178, (23,24)]. Furthermore, IgG antibodies can form ordered hexamers upon binding to their antigen on cell surfaces. These hexamers efficiently bind the hexavalent complement component C1q, the first step in the classical pathway of complement activation (43,44). The structure of C_{44}Mab-46-mG_{2a}-CD44 complex may provide the adequate access of complements to exert CDC.

Complement has been considered as an adjunctive component that potentiates the antibody-mediated cytolytic effects. However, complement is currently considered an essential effector of tumor cytotoxic responses of antibody-based immunotherapy, which is guiding new therapeutic options (41). An increasing body of evidence suggests that complement plays critical roles in not only mAb-mediated tumor cytolysis but also several immunomodulatory functions in tumor immunosurveillance and antitumor immunity (45,46). The complicated crosstalk of complement effectors with cellular pathways that drive B cell and T cell responses influences T helper/effector T cell survival, differentiation and B cell activation. Therefore, the involvement of complement in our experimental system and/or immunocompetent mouse models should be investigated in future studies.

Most therapeutic mAbs exhibit adverse effects by recognizing antigens in normal cells (47). Clinical trials of an anti-CD44v6 mAb (BIWA-4) bivatuzumab-mertansine drug conjugate to solid tumors failed because of the skin toxicities (17,18). Therefore, cancer-selective or specific mAbs would reduce the adverse effects. Cancer-specific mAbs (CasMabs) against HER2 [H_2Mab-214 (48) and H_2Mab-250 (49)] have been developed by the authors and the reactivity to cancer and normal cells has been evaluated using flow cytometry. The antitumor effect in mouse xenograft models has been also reported using a mouse IgG_{2a} or human IgG_1 types recombinant mAbs (50). Some anti-CD44 mAbs which exhibit cancer specificity have been reported (51). Among them, the 4C8

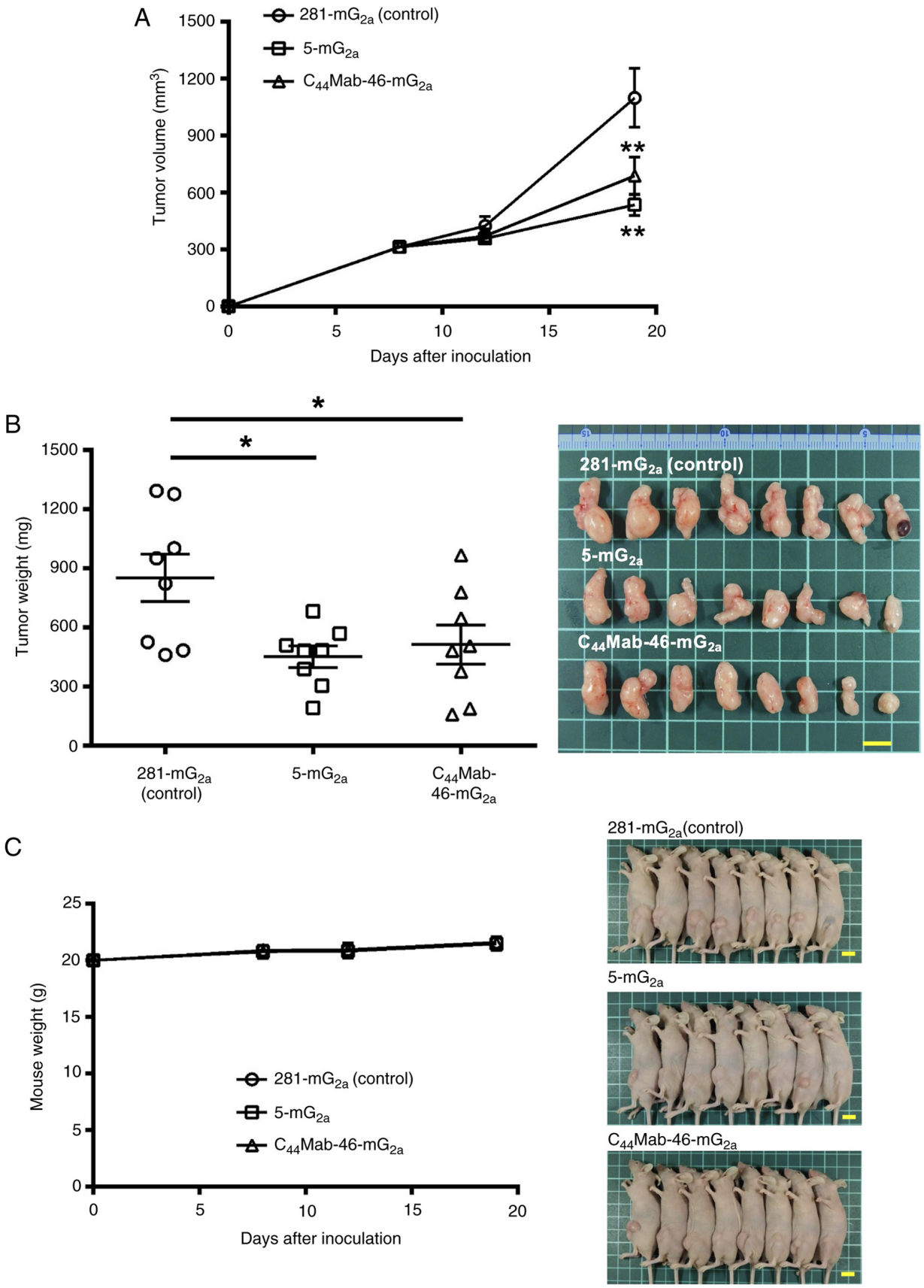

Figure 5. Antitumor activity of 5-mG_{2a} and C_{44}Mab-46-mG_{2a} against KYSE770 xenograft tumor. (A) Measurement of tumor volume in KYSE770 xenograft. KYSE770 cells ($5x10^6$ cells) were injected into mice subcutaneously. On day 8, 500 μg of 5-mG_{2a} and C_{44}Mab-46-mG_{2a} or control mouse IgG_{2a} (281-mG_{2a}) were injected into mice intraperitoneally. On day 13, additional antibodies were injected. On days 8, 12, and 19 following the inoculation, the tumor volume was measured. Values are presented as the mean ± SEM. **P<0.01; two-way ANOVA with Sidak's multiple comparisons test. (B) The weight (left) and appearance (right) of the excised KYSE770 xenografts on day 19. Values are presented as the mean ± SEM. *P<0.05; one-way ANOVA with Tukey's multiple comparisons test. (C) The body weight (left) and appearance (right) of control mouse IgG_{2a}, 5-mG_{2a} and C_{44}Mab-46-mG_{2a}-treated mice. Scale bar, 1 cm. mAb, monoclonal antibody.

mAb recognizes aberrantly *O*-glycosylated CD44v6 with Tn (GalNAcα1-*O*-Ser/Thr) antigen. The 4C8 chimeric antigen receptor (CAR)-T cells demonstrated target-specific cytotoxicity *in vitro,* significant tumor regression, and prolonged survival *in vivo* (52). In our CasMab development against CD44, already established anti-CD44 mAbs were screened by comparing the reactivity against cancer and normal cells. The CasMabs against CD44 could be applicable for designing modalities such as antibody-drug conjugates and CAR-T cells.

Acknowledgements

The authors thank Mr Shun-ichi Ohba and Ms Akiko Harakawa [Institute of Microbial Chemistry (BIKAKEN), Numazu, the Microbial Chemistry Research Foundation] for technical assistance with animal experiments.

Funding

The present study was supported in part by Japan Agency for Medical Research and Development (AMED) (grant nos. JP23ama121008, JP24am0521010, JP23bm1123027 and JP23ck0106730) and by the Japan Society for the Promotion of Science (JSPS) Grants-in-Aid for Scientific Research (KAKENHI) (grant nos. 22K06995, 21K20789, 21K07168 and 22K07224).

Availability of data and materials

The data generated in the present study are included in the figures and/or tables of this article.

Authors' contributions

KI, HS, TO, TN, MY, GL and TT performed the experiments. MK, MKK and YKato designed the experiments. KI, HS, AO, YKatori and YKato engaged the analysis and interpretation of data. KI, HS, and YKato wrote the manuscript. HS and YKato confirm the authenticity of all the raw data. All authors read and approved the final version of the manuscript.

Ethics approval and consent to participate

Animal experiments were approved (approval nos. 2023-037 and 2023-054) by the Institutional Committee for Experiments of the Institute of Microbial Chemistry (Numazu, Japan).

Patient consent for publication

Not applicable.

Competing interests

The authors declare that they have no competing interests.

References

1. Ponta H, Sherman L and Herrlich PA: CD44: From adhesion molecules to signalling regulators. Nat Rev Mol Cell Biol 4: 33-45, 2003.
2. Zöller M: CD44: Can a cancer-initiating cell profit from an abundantly expressed molecule? Nat Rev Cancer 11: 254-267, 2011.
3. Prochazka L, Tesarik R and Turanek J: Regulation of alternative splicing of CD44 in cancer. Cell Signal 26: 2234-2239, 2014.
4. Guo Q, Yang C and Gao F: The state of CD44 activation in cancer progression and therapeutic targeting. FEBS J 289: 7970-7986, 2022.
5. Zöller M: CD44, hyaluronan, the hematopoietic stem cell, and leukemia-initiating cells. Front Immunol 6: 235, 2015.
6. Hassn Mesrati M, Syafruddin SE, Mohtar MA and Syahir A: CD44: A multifunctional mediator of cancer progression. Biomolecules 11: 1850, 2021.
7. Cirillo N: The hyaluronan/CD44 axis: A double-edged sword in cancer. Int J Mol Sci 24: 15812, 2023.
8. Liu Y, Wu T, Lu D, Zhen J and Zhang L: CD44 overexpression related to lymph node metastasis and poor prognosis of pancreatic cancer. Int J Biol Markers 33: 308-313, 2018.
9. Tao Y, Li H, Huang R, Mo D, Zeng T, Fang M and Li M: Clinicopathological and prognostic significance of cancer stem cell markers in ovarian cancer patients: Evidence from 52 studies. Cell Physiol Biochem 46: 1716-1726, 2018.
10. Li L, Hao X, Qin J, Tang W, He F, Smith A, Zhang M, Simeone DM, Qiao XT, Chen ZN, *et al*: Antibody against CD44s inhibits pancreatic tumor initiation and postradiation recurrence in mice. Gastroenterology 146: 1108-1118, 2014.
11. Zhang S, Wu CC, Fecteau JF, Cui B, Chen L, Zhang L, Wu R, Rassenti L, Lao F, Weigand S and Kipps TJ: Targeting chronic lymphocytic leukemia cells with a humanized monoclonal antibody specific for CD44. Proc Natl Acad Sci USA 110: 6127-6132, 2013.
12. Vey N, Delaunay J, Martinelli G, Fiedler W, Raffoux E, Prebet T, Gomez-Roca C, Papayannidis C, Kebenko M, Paschka P, *et al*: Phase I clinical study of RG7356, an anti-CD44 humanized antibody, in patients with acute myeloid leukemia. Oncotarget 7: 32532-32542, 2016.
13. Menke-van der Houven van Oordt CW, Gomez-Roca C, van Herpen C, Coveler AL, Mahalingam D, Verheul HM, van der Graaf WT, Christen R, Rüttinger D, Weigand S, *et al*: First-in-human phase I clinical trial of RG7356, an anti-CD44 humanized antibody, in patients with advanced, CD44-expressing solid tumors. Oncotarget 7: 80046-80058, 2016.
14. Todaro M, Gaggianesi M, Catalano V, Benfante A, Iovino F, Biffoni M, Apuzzo T, Sperduti I, Volpe S, Cocorullo G, *et al*: CD44v6 is a marker of constitutive and reprogrammed cancer stem cells driving colon cancer metastasis. Cell Stem Cell 14: 342-356, 2014.
15. Verel I, Heider KH, Siegmund M, Ostermann E, Patzelt E, Sproll M, Snow GB, Adolf GR and van Dongen GA: Tumor targeting properties of monoclonal antibodies with different affinity for target antigen CD44V6 in nude mice bearing head-and-neck cancer xenografts. Int J Cancer 99: 396-402, 2002.
16. Orian-Rousseau V and Ponta H: Perspectives of CD44 targeting therapies. Arch Toxicol 89: 3-14, 2015.
17. Tijink BM, Buter J, de Bree R, Giaccone G, Lang MS, Staab A, Leemans CR and van Dongen GA: A phase I dose escalation study with anti-CD44v6 bivatuzumab mertansine in patients with incurable squamous cell carcinoma of the head and neck or esophagus. Clin Cancer Res 12: 6064-6072, 2006.
18. Riechelmann H, Sauter A, Golze W, Hanft G, Schroen C, Hoermann K, Erhardt T and Gronau S: Phase I trial with the CD44v6-targeting immunoconjugate bivatuzumab mertansine in head and neck squamous cell carcinoma. Oral Oncol 44: 823-829, 2008.
19. Casucci M, Nicolis di Robilant B, Falcone L, Camisa B, Norelli M, Genovese P, Gentner B, Gullotta F, Ponzoni M, Bernardi M, *et al*: CD44v6-targeted T cells mediate potent antitumor effects against acute myeloid leukemia and multiple myeloma. Blood 122: 3461-3472, 2013.
20. Porcellini S, Asperti C, Corna S, Cicoria E, Valtolina V, Stornaiuolo A, Valentinis B, Bordignon C and Traversari C: CAR T cells redirected to CD44v6 control tumor growth in lung and ovary adenocarcinoma bearing mice. Front Immunol 11: 99, 2020.
21. Yamada S, Itai S, Nakamura T, Yanaka M, Kaneko MK and Kato Y: Detection of high CD44 expression in oral cancers using the novel monoclonal antibody, C_{44}Mab-5. Biochem Biophys Rep 14: 64-68, 2018.
22. Goto N, Suzuki H, Tanaka T, Asano T, Kaneko MK and Kato Y: Development of a novel Anti-CD44 monoclonal antibody for multiple applications against esophageal squamous cell carcinomas. Int J Mol Sci 23: 5535, 2022.

23. Takei J, Asano T, Suzuki H, Kaneko MK and Kato Y: Epitope mapping of the anti-CD44 monoclonal antibody (C44Mab-46) using alanine-scanning mutagenesis and surface plasmon resonance. Monoclon Antib Immunodiagn Immunother 40: 219-226, 2021.
24. Asano T, Kaneko MK, Takei J, Tateyama N and Kato Y: Epitope mapping of the anti-CD44 monoclonal antibody (C_{44}Mab-46) using the REMAP method. Monoclon Antib Immunodiagn Immunother 40: 156-161, 2021.
25. Asano T, Kaneko MK and Kato Y: Development of a novel epitope mapping system: RIEDL insertion for epitope mapping method. Monoclon Antib Immunodiagn Immunother 40: 162-167, 2021.
26. Suzuki H, Kitamura K, Goto N, Ishikawa K, Ouchida T, Tanaka T, Kaneko MK and Kato Y: A Novel anti-CD44 variant 3 monoclonal antibody C_{44}Mab-6 was established for multiple applications. Int J Mol Sci 24: 8411, 2023.
27. Suzuki H, Tanaka T, Goto N, Kaneko MK and Kato Y: Development of a novel anti-CD44 variant 4 monoclonal antibody C_{44}Mab-108 for immunohistochemistry. Curr Issues Mol Biol 45: 1875-1888, 2023.
28. Kudo Y, Suzuki H, Tanaka T, Kaneko MK and Kato Y: Development of a novel Anti-CD44 variant 5 monoclonal antibody C_{44}Mab-3 for multiple applications against pancreatic carcinomas. Antibodies (Basel) 12: 31, 2023.
29. Ejima R, Suzuki H, Tanaka T, Asano T, Kaneko MK and Kato Y: Development of a novel Anti-CD44 variant 6 monoclonal antibody C_{44}Mab-9 for multiple applications against colorectal carcinomas. Int J Mol Sci 24: 4007, 2023.
30. Suzuki H, Ozawa K, Tanaka T, Kaneko MK and Kato Y: Development of a novel anti-CD44 variant 7/8 monoclonal antibody, C_{44}Mab-34, for multiple applications against oral carcinomas. Biomedicines 11: 1099, 2023.
31. Tawara M, Suzuki H, Goto N, Tanaka T, Kaneko MK and Kato Y: A novel anti-CD44 variant 9 monoclonal antibody C_{44}Mab-1 was developed for immunohistochemical analyses against colorectal cancers. Curr Issues Mol Biol 45: 3658-3673, 2023.
32. Ishikawa K, Suzuki H, Kaneko MK and Kato Y: Establishment of a novel anti-CD44 variant 10 monoclonal antibody C_{44}Mab-18 for immunohistochemical analysis against oral squamous cell carcinomas. Curr Issues Mol Biol 45: 5248-5262, 2023.
33. Li G, Suzuki H, Ohishi T, Asano T, Tanaka T, Yanaka M, Nakamura T, Yoshikawa T, Kawada M, Kaneko MK and Kato Y: Antitumor activities of a defucosylated anti-EpCAM monoclonal antibody in colorectal carcinoma xenograft models. Int J Mol Med 51: 18, 2023.
34. Nanamiya R, Suzuki H, Takei J, Li G, Goto N, Harada H, Saito M, Tanaka T, Asano T, Kaneko MK and Kato Y: Development of monoclonal antibody 281-mG_{2a}-f against golden hamster podoplanin. Monoclon Antib Immunodiagn Immunother 41: 311-319, 2022.
35. Queiroz AL, Dantas E, Ramsamooj S, Murthy A, Ahmed M, Zunica ERM, Liang RJ, Murphy J, Holman CD, Bare CJ, *et al*: Blocking ActRIIB and restoring appetite reverses cachexia and improves survival in mice with lung cancer. Nat Commun 13: 4633, 2022.
36. Yamada S, Kaneko MK, Nakamura T, Ichii O, Konnai S and Kato Y: Development of mPMab-1, a mouse-rat chimeric antibody against mouse podoplanin. Monoclon Antib Immunodiagn Immunother 36: 77-79, 2017.
37. Garvin D, Stecha P, Gilden J, Wang J, Grailer J, Hartnett J, Fan F, Cong M and Cheng ZJ: Determining ADCC activity of antibody-based therapeutic molecules using two bioluminescent reporter-based bioassays. Curr Protoc 1: e296, 2021.
38. Takei J, Kaneko MK, Ohishi T, Hosono H, Nakamura T, Yanaka M, Sano M, Asano T, Sayama Y, Kawada M, *et al*: A defucosylated anti-CD44 monoclonal antibody 5-mG2a-f exerts antitumor effects in mouse xenograft models of oral squamous cell carcinoma. Oncol Rep 44: 1949-1960, 2020.
39. Birzele F, Voss E, Nopora A, Honold K, Heil F, Lohmann S, Verheul H, Le Tourneau C, Delord JP, van Herpen C, *et al*: CD44 isoform status predicts response to treatment with anti-CD44 antibody in cancer patients. Clin Cancer Res 21: 2753-2762, 2015.
40. Golay J and Taylor RP: The role of complement in the mechanism of action of therapeutic anti-cancer mAbs. Antibodies (Basel) 9: 58, 2020.
41. Reis ES, Mastellos DC, Ricklin D, Mantovani A and Lambris JD: Complement in cancer: Untangling an intricate relationship. Nat Rev Immunol 18: 5-18, 2018.
42. Galon J and Bruni D: Approaches to treat immune hot, altered and cold tumours with combination immunotherapies. Nat Rev Drug Discov 18: 197-218, 2019.
43. Hiemstra IH, Santegoets KCM, Janmaat ML, De Goeij BECG, Ten Hagen W, van Dooremalen S, Boross P, van den Brakel J, Bosgra S, Andringa G, *et al*: Preclinical anti-tumour activity of HexaBody-CD38, a next-generation CD38 antibody with superior complement-dependent cytotoxic activity. EBioMedicine 93: 104663, 2023.
44. de Jong RN, Beurskens FJ, Verploegen S, Strumane K, van Kampen MD, Voorhorst M, Horstman W, Engelberts PJ, Oostindie SC, Wang G, *et al*: A novel platform for the potentiation of therapeutic antibodies based on antigen-dependent formation of IgG hexamers at the cell surface. PLoS Biol 14: e1002344, 2016.
45. Schmudde I, Laumonnier Y and Köhl J: Anaphylatoxins coordinate innate and adaptive immune responses in allergic asthma. Semin Immunol 25: 2-11, 2013.
46. Carroll MC and Isenman DE: Regulation of humoral immunity by complement. Immunity 37: 199-207, 2012.
47. Gogia P, Ashraf H, Bhasin S and Xu Y: Antibody-drug conjugates: A review of approved drugs and their clinical level of evidence. Cancers (Basel) 15: 3886, 2023.
48. Arimori T, Mihara E, Suzuki H, Ohishi T, Tanaka T, Kaneko MK, Takagi J and Kato Y: Locally misfolded HER2 expressed on cancer cells is a promising target for development of cancer-specific antibodies. Structure 32: 536-549.e5, 2024.
49. Kaneko MK, Suzuki H and Kato Y: Establishment of a novel cancer-specific anti-HER_2 monoclonal antibody H_2Mab-250/H_2CasMab-2 for breast cancers. Monoclon Antib Immunodiagn Immunother 43: 35-43, 2024.
50. Kaneko MK, Suzuki H, Ohishi T, Nakamura T, Tanaka T and Kato Y: A cancer-specific monoclonal antibody against HER2 exerts antitumor activities in human breast cancer xenograft models. Int J Mol Sci 25: 1941, 2024.
51. Lodewijk I, Dueñas M, Paramio JM and Rubio C: CD44v6, STn & O-GD2: Promising tumor associated antigens paving the way for new targeted cancer therapies. Front Immunol 14: 1272681, 2023.
52. Aasted MKM, Groen AC, Keane JT, Dabelsteen S, Tan E, Schnabel J, Liu F, Lewis HS, Theodoropulos C, Posey AD and Wandall HH: Targeting solid cancers with a cancer-specific monoclonal antibody to surface expressed aberrantly O-glycosylated proteins. Mol Cancer Ther 22: 1204-1214, 2023.